Geothermics 87 (2020) 101848

Contents lists available at ScienceDirect

Geothermics

journal homepage: www.elsevier.com/locate/geothermics

Modeling study of deep direct use geothermal on the West Virginia university campus-morgantown, WV

Yingqi Zhang[a,*], Nagasree Garapati[b], Christine Doughty[a], Pierre Jeanne[a]

[a] Lawrence Berkeley National Laboratory, Berkeley, United States
[b] Department of Chemical and Biomedical Engineering, West Virginia University, United States

ARTICLE INFO

Keywords:
Deep Direct-use geothermal
Numerical simulations
Prediction uncertainty
Heterogeneity

ABSTRACT

To reduce the geothermal exploration risk, a feasibility study is performed for a deep direct-use (DDU) system proposed at the West Virginia University (WVU) Morgantown campus. This study applies numerical simulations to investigate reservoir impedance and thermal production. Because of the great depth of the geothermal reservoir, few data are available to characterize reservoir features and properties. As a result, the study focuses on the following three aspects: 1. model choice for predicting reservoir impedance and thermal breakthrough: after investigating three potential models (one single permeability model and two dual permeability models) for flow through fractured rock, it is decided only the single permeability model is needed; 2. well placement (horizontal vs. vertical) options: horizontal well placement seems to be more robust to heterogeneity and the impedance is more acceptable; 3. Prediction uncertainty: the most influential parameters are identified using a First-Order-Second-Moment uncertainty propagation analysis, and the uncertain range of the model predictions is estimated by performing a Monte Carlo simulation. Heterogeneity has a large impact on the prediction, therefore, heterogeneity is included in the predictive model and uncertainty analysis. The numerical model results and uncertainty analysis will be used for further economic studies.

1. Objective

Heating is the largest energy use associated within the building sector, which accounts for 40 % of U.S. energy demand (Tester, 2015). Extracting heat from geothermal reservoirs for direct use not only diversifies energy supply options but also helps reaching clean energy goals. As part of the Department of Energy (DOE)'s Deep Direct-Use (DDU) research program, a Geothermal District Heating and Cooling system for West Virginia University (WVU) Morgantown campus has been proposed to replace the current coal-fired steam heating and cooling system. The idea of direct-use of geothermal is not new, for example, in Iceland 90 % of homes are heated with geothermal systems (Jóhannesson, 2015). A typical method to understand a proposed geothermal system and reduce exploration risk is to perform subsurface modeling to predict reservoir impedance as well as thermal behavior for designs of interest. However, DDU projects often have challenges because of the great depth of the geothermal reservoir, which is at about 3 km for the WVU project. The challenges mainly come from the unknown reservoir features and properties, which make it difficult to build a predictive model for understanding the system behavior, which is important in determining technical and economic feasibilities. Most studies using numerical models for deep direct-use (for examples, Major et al., 2018) have not addressed these challenges.

Although a complete evaluation of the WVU project would include economic analysis, the investigation here focuses on subsurface processes, and in particular, addresses the following questions:

- What are the possible reservoir pressures and how does the production temperature evolve over time? What is an appropriate model to predict system behavior?
- What well placement is best for such a system? For this feasibility modeling study, a pair of wells with one injector and one producer is considered. Well placement includes the option of using horizontal wells or vertical wells; as well as choosing the distance between the injection and production wells. In this study, we will mainly demonstrate the difference in production temperature and reservoir impedance (RI) between horizontal and vertical well layouts so results can be used as a basis for well placement design. In terms of well pair distance, the farther apart the two wells are, the longer it takes to have thermal breakthrough at the production well. However, longer distance also results in higher pressure difference between the injection and pressure wells. The detailed simulation

* Corresponding author at: Energy Geosciences Division, Lawrence Berkeley National Laboratory, One Cyclotron, MS 74-316C, Berkeley, CA 94720, United States.
E-mail address: yqzhang@lbl.gov (Y. Zhang).

https://doi.org/10.1016/j.geothermics.2020.101848
Received 17 December 2019; Received in revised form 26 February 2020; Accepted 30 March 2020
Available online 11 April 2020
0375-6505/

results can be found in Garapati et al. (2019).

- What is the uncertainty in the model prediction? What are the most valuable data to be collected for reducing the uncertainty in the prediction?

The paper is organized as follows: we will first introduce the site and geology; then we will describe the model options considered and the model used for the study; after providing the model results to address the question of well placement, we will present an analysis of prediction uncertainty, followed by concluding remarks.

2. Site description and geological information

Morgantown campus of WVU is located in a region with elevated heat flows in north-central West Virginia (Cornell University, 2017). The geology of the proposed site is assumed to be similar to the geology predicted from nearby well logs penetrating the Marcellus shale and Tuscarora sandstone in Preston and Harrison counties, for the given depth range. The depth of interest for the geothermal resource is between 2600 m and 2940 m, where the Tuscarora sandstones are located, with a thickness of approximately 100 m. Based on the resistivity logs and gas production histories in the Tuscarora, significant porosity and permeability is expected. Fracture flow is assumed to be important since the matrix permeability is thought to be too low to sustain the historic gas production rates. However, detailed knowledge of the fracture network is limited. A previous study (Ryder and Zagorski, 2003) indicates that most commonly the fractures are vertical to subvertical, and are either open or incompletely mineralized by euhedral quartz crystals, calcite, hematite, anhydrite, and gypsum. Core analysis for measurements spanning a 83 m interval of the Preston-119 well located about 50 km SSE of Morgantown has been performed (McDowell, 2018). The results indicate that the permeabilities of the vertical fractures in the upper 2/3rd of the Tuscarora formation are on the order of 60 mD and for the lower 1/3rd of the formation are about 4 mD. Matrix permeability is on the order of 2.4 mD, without much variation with depth.

The heat map of the region can be found in Garapati et al. (2019). The temperature at the depth of the Tuscarora sandstone in Morgantown was estimated using local corrected bottom-hole temperature (BHT) data (Cornell University, 2017; correction equations are described in Whealton et al., 2015) and a fiber optic distributed temperature log taken within 5 km of the WVU campus (MSEEL, 2018). The temperature log provides data to a depth of about 2.2 km in Morgantown. Prediction of temperatures at greater depths is informed by local BHTs using the methods described in Smith (2016) (also in Cornell University, 2017). The initial temperature used in this study is calculated using a surface temperature of 13.2 °C and geothermal gradient of 26 °C/km, resulting in a reservoir temperature in the range between 80 ~ 90 °C at reservoir depth.

3. Potential numerical models

The numerical simulation software used in the study is iTOUGH2/eos1 (Finsterle, 2004; Finsterle et al., 2008). TOUGH2 (Pruess et al., 1999) code is a simulator for multiphase, multicomponent, non-isothermal flows in fractured-porous media. The iTOUGH2 simulation–optimization code, wrapped around the TOUGH2 code, provides inverse modeling capabilities as well as formal (local and global) sensitivity and uncertainty propagation analyses for the TOUGH2 code. Among the various equation-of-state (eos) modules, eos1 was specifically developed for geothermal applications. Module eos1 considers two fluid phases – liquid and gas – and one mass component – water.

3.1. Numerical model domain

A 3-D geological model (shown in Fig. 1a) centered on the proposed well location was constructed with the 3-D GeoModeller GMS (Aquaveo, 2013), based on three geological studies: (1) through the Appalachian Basin (Ryder et al., 2009), cross sections C-C', D–D' and E-E', (2) on the Trenton-Black River reservoirs in West Virginia (Patchen et al., 2006), and (3) on the Tuscarora sandstone at the Morgantown region (McCleery et al., 2018). Only the Tuscarora formation is included in the numerical model for two reasons: (1) the permeabilities above and below the Tuscarora formation are so low that the fluid flow into or out of the Tuscarora formation is limited. In addition, since there is no knowledge that active fractures exist to connect the Tuscarora formation and the upper/lower confining formations, this minimal flow is ignored and in the model it is assumed there is no hydraulic connection between the Tuscarora formation and the upper/lower confining formation; (2) the heat exchange at the top/bottom of the Tuscarora formation can be modeled using a semi-analytical solution (Pruess et al., 1999). After some initial simulations using a numerical model with a horizontal extent of 17 km in each direction, and a pair of vertical wells 500 m apart, it was determined that the numerical model domain can be reduced to 5 km × 5 km horizontally (horizontal domain is shown in Fig. 1b), as the pressure change at 2.5 km away from the wells is negligible.

3.2. Potential models for fracture/matrix fluid flow

There are different ways to model flow in fractured media. A basic method is to use a single continuum model with fracture permeabilities and matrix porosity. However, a more accurate description can be achieved by either using a multiple interacting continua (MINC) approach (Pruess et al., 1999) or modeling a discrete fracture network (DFN) explicitly if there is information on individual large fractures. Since there is no information on any discrete fractures in the region of interest, it is determined to investigate both a single-permeability (single-K) model and dual-permeability model (dual-K) model (which is a simplified version of the MINC approach). From the Preston-119 well core analysis (McDowell, 2018), aperture and permeability distribution along depth are plotted to identify fractures. Based on the fracture histograms, two dual-K models are considered; (1) one with a fracture spacing of 0.3 m and fracture volume fraction of 1.5×10^{-3}; and (2) a second dual-K model similar to the previous one but with only 10 % of the fractures contributing to flow, representing a more extreme case in which the flow is only conducted by the portion of larger fractures. The fracture properties of the two dual-K models are determined from the fracture and matrix permeability distribution along the vertical depth of the core (McDowell, 2018). Model properties are listed in Table 1.

3.3. Model results

All simulations are run for a 60-year period, with an injection/production rate of 15 kg/s. which is based on surface peak demand during winter season. For simplicity, it is assumed that the water is injected at the surface temperature (13.2 °C). Initially temperatures in both the wellbore and formation follow the geothermal gradient, i.e., temperature is 13.2 °C at the surface and gradually increases with depth, reaching ~87 °C at the well bottom. As the injected water travels down towards the reservoir, it is gradually heated up by the warmer formation around it. At the same time, the formation around the well is gradually cooled down by the colder injected fluid, so the heating by the formation gets less and less effective with time. A simulation containing only the injection well using a semi-analytical solution (Zhang et al., 2011) has been applied to understand the importance of the formation heating on the wellbore. Using a well with a 10 cm radius, the temperature at the well bottom after 1 hour, 1 day, and 1 month of 13.2 °C water injection are 48 °C, 24 °C, and 17 °C, respectively. Given the uncertainty in the temperature of actual injected water, and the simulation time frame (60 years), simulating this effect is not important and therefore can be neglected. However, it is likely that the produced

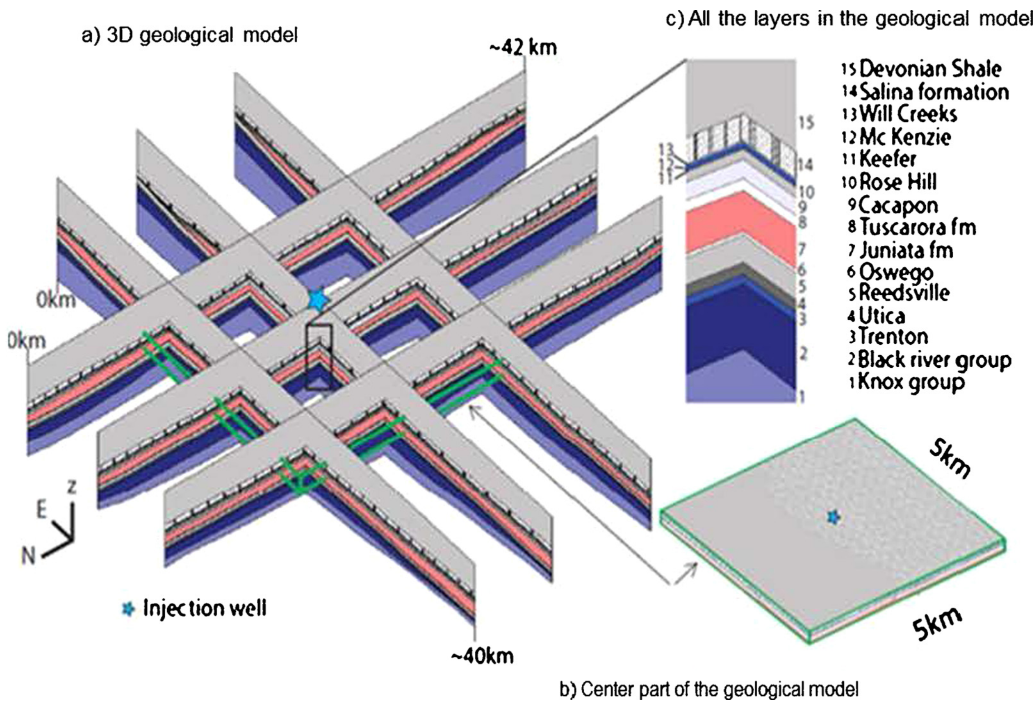

Fig. 1. a) 3D geological model centered on the proposed well location as the basis for a 3-D numerical model; b) the horizontal domain used for the numerical model; c) geological layers above and below the Tuscarora formation. Note that the Tuscarora formation in c) is the only formation included in the numerical model.

water is re-injected and the actual injected water has a much higher temperature. How this may influence the results will be discussed in the next section.

For these preliminary modeling studies, regional groundwater flow is presumed to be negligible. Typically, for very deep, highly saline aquifers such as the Tuscarora formation, regional groundwater flow is much smaller than in shallower fresh-water aquifers with more communication to surface hydrological processes (Burns et al., 2018). Moreover, Ryder and Zagorski (2003) noted pressures often vary between overpressured, hydrostatic, and underpressured in different regions of aquifers within the Lower Silurian Regional Accumulation (which includes the Tuscarora formation), indicating poor continuity of these aquifers, again suggesting low regional groundwater flow. As pressure data become available with the drilling of wells into the Tuscarora formation, regional hydraulic gradient can be determined and regional groundwater flow estimated and included in the model if deemed necessary. It should be noted that thermal velocity (how fast the plume of cool water moves) is typically smaller than the actual groundwater velocity by a factor on the order of the porosity. If thermal velocity is shown to be significant, the orientation of the injection well/production well pair can be chosen to minimize negative effects such as premature breakthrough.

Here, two types of well placements are considered and discussed: a pair of vertical wells 500 m apart, and a pair of horizontal wells 500 m apart. Similar well placements with other well separation distances were discussed by Garapati et al. (2019). Although the reservoir depth changes over the numerical model domain, the reservoir depths are the same at the two well locations for scenarios with well separations less than 1000 m. Thus, it is reasonable to assume that the production well is at the same depth as the injection well. The production well is set at a constant bottom-hole pressure to achieve a production rate of approximately 15 kg/s.

3.3.1. Vertical well layout

For the case with two vertical wells, 500 m apart, the thermal breakthrough happens after 20 years of operation, in all three models, as shown in Fig. 2. There is hardly any difference observed between the two dual-K models; at the end of 60 years, the production temperature is about 79 °C using the single-K model, and 80 °C using the dual-K models. Given the injected water is at 13.2 °C, the 1 °C difference over 60 years is considered insignificant. The temperature distributions at different times as shown in Fig. 3 also show no visual difference among the models. To examine why the temperatures in the formation and at the production wells are not sensitive to the model choice, several hypothesis can be proposed:

1 In the dual-K models, the difference between matrix permeability and fracture permeability is not significant (i.e., only about one order of magnitude). In contrast, the fracture volume is only on the order of 0.015 ~ 0.15 % of the entire rock mass. Therefore, the matrix potentially carries a significant amount of fluid flow. If the heat transfer regime in the dual-K model becomes convection dominated (i.e., fluid flow through the matrix is so large that temperatures in the fractures and matrix are similar and conductive heat

Table 1
Fracture and matrix properties used in the three models.

Model	Permeability (mD)				Porosity		Fracture spacing (m)	Fracture Volume Fraction
	Upper 2/3 Fracture	Matrix	Lower 1/3 Fracture	Matrix	Fracture	Matrix		
Single K	60		4		0.08		N/A	N/A
First Dual K	60	2.4	4	2.4	0.99	0.08	0.3	1.5×10^{-3}
Second Dual K	60	2.4	4	2.4	0.99	0.08	3.0	1.5×10^{-4}

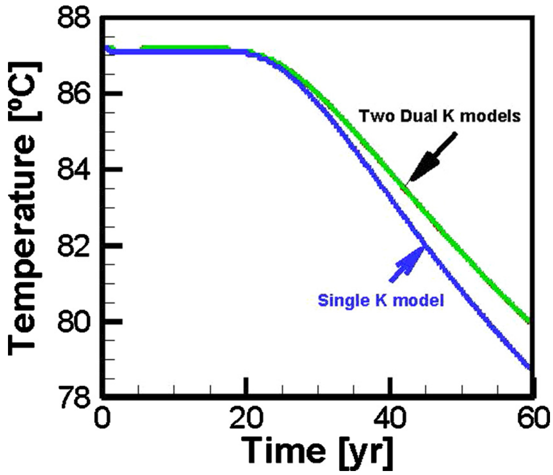

Fig. 2. Thermal breakthrough curve at the production well with two vertical wells with 500 m apart layout. The temperature is about 79 °C from the single K model and 80 °C from the two dual K models at the end of 60 years. The difference from the two types of model is considered insignificant given the injected temperature is 13.2 °C.

transfer between the fracture and the matrix is negligible), as in the single-K model, this would explain why the dual-K models had very similar results to the single-K model. To test the hypothesis, we first decreased the matrix permeability to 2.4E-5 mD for the dual-K model. We examined the flow between matrix blocks, flow between matrix and fracture blocks, and flow between fracture blocks in the dual-K model. Any flow involving matrix blocks is negligible compared to the flow between fracture blocks. However, the thermal breakthrough curves (BTCs) are still very similar between the single-K model and dual-K models, i.e., the curves are similar to the ones shown in Fig. 2. This means the hypothesis of a heat transfer regime dominated by convection cannot explain the similarity in the BTC predictions from the three models.

2 The previous investigation implies that heat conduction is still very effective in the dual-K models. Re-examining the fracture parameter sets for both dual-K models, we suspected the similar thermal breakthrough behaviors between the single-K and dual-K models is due to the fracture spacing choice in the two dual-K models (0.3 m and 3 m). To investigate, we first calculate the thermal penetration length ($k\sqrt{Dt}$, in which the thermal diffusivity D is $\frac{k_c}{\rho C_p}$, k_c — thermal conductivity, ρ — density, and Cp — heat capacity; t is time; and k is a loosely defined constant, here we use $k = 2$) for three cases with different matrix thermal conductivities as shown in Table 2. The matrix thermal conductivity in our model is 2 W/m °C,correspondingto a thermal penetration of 10 m at one year, which is much larger than the fracture spacing used in both dual-K models (i.e., 0.3 m and 3 m). That is why the dual-K and single-K model results are very similar given the time scale we have for our simulations.

Table 2
Thermal penetration length $L = 2\sqrt{Dt}$ for different thermal conductivities kc.

(W/ m °c)	$kc = 1$	$kc = 2$	$kc = 3$
Time (year)	L (m)	L (m)	L (m)
1	7.1	10.0	12.3
10	22.5	31.8	38.9
60	55.0	77.8	95.3

To further confirm this hypothesis, we examined the temperature distributions for both fractures and matrix in the dual-K model with a fracture spacing of 0.3 m. There is no difference between the temperature in fracture elements and temperature in corresponding matrix elements anywhere in the model.

Lastly, we built a new dual-K model (Mtest) with fracture spacing of 100 m. The purpose of this model is not to simulate what happens at the WVU site; it is more to confirm our hypothesis, and help to understand model choice. The goal of using this large fracture spacing is to simulate large sparse fractures that can have real dual-K effects, and to compare with our previous models to see if the choice makes a difference.

For the Mtest model, the temperature in fractures is much colder than the temperature in the matrix around the injection well after 1 year, as shown in Fig. 4 (notice only the model domain around injection well, i.e., 100 m in each direction, is shown). This temperature difference between matrix and fractures is seen in early years, then gradually diminishes as the heat in matrix blocks is exhausted, as shown in Fig. 5. Fig. 5 shows temperature in both continua at 20 years, 40 years, and 60 years, with a large difference at 20 years, that gradually reduces and almost diminishes at the end of 60 years.

Summarizing the analysis, the large distance between the injection/ production wells (in all potential scenarios) and radial geometry of the injected cold-water plume lead to a large volume of matrix being accessed by fracture flow. Given the long residence time and relatively small fracture spacing even in a more conservative scenario, the heat exchange between fracture and matrix is dominated by the matrix volume rather than heat exchange area between fracture and matrix (Zhou et al., 2019), therefore the dual-K models behave similarly to a porous medium.

The above analysis lead to the conclusion that for this particular scenario, the thermal behavior at the production well is not sensitive to the model choices (i.e., between a single-K and dual-K models with different parameters). This may not be the case if the system contains very large sparse fractures, but as yet there is no data to support this.

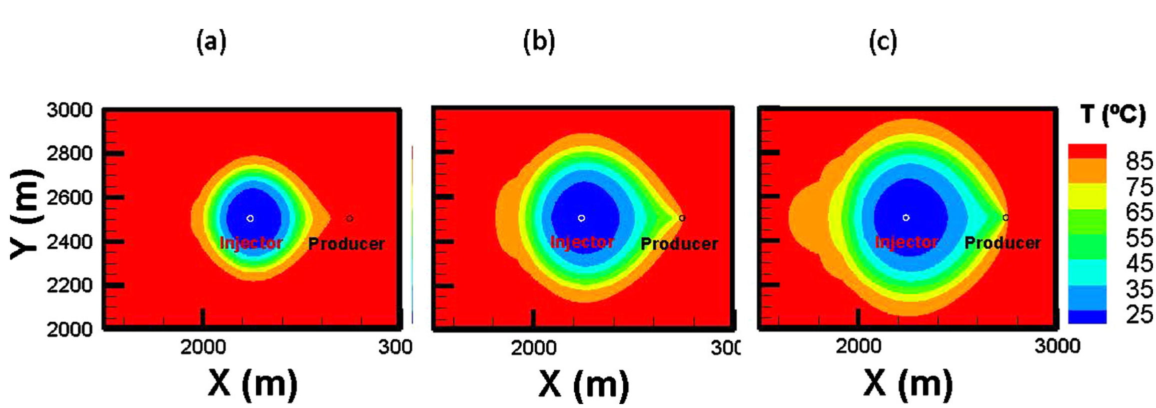

Fig. 3. Temperature distribution (in ºC) on an XY plane at an elevation where injection/production wells are perforated at (a) 20 years; (b) 40 years; and (c) 60 years for the single-K model. Results from the two dual-K models are very similar, with no visual difference, therefore, are not shown here.

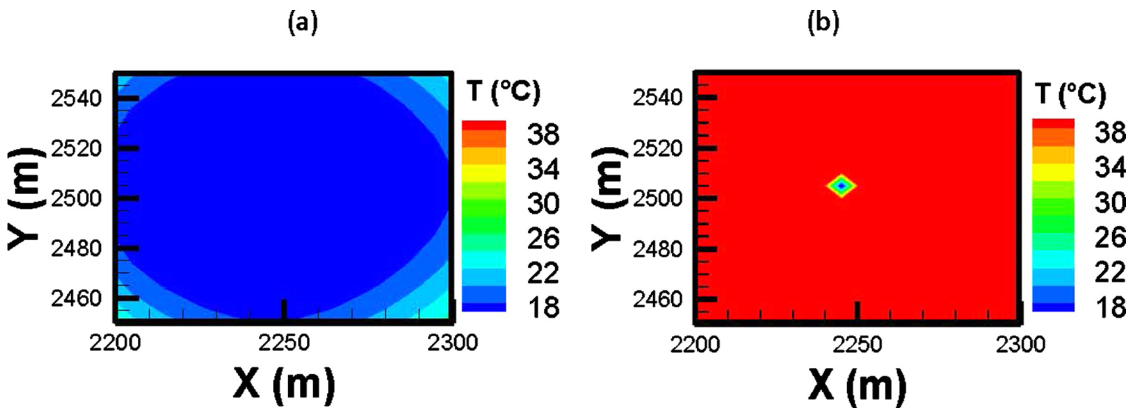

Fig. 4. Temperature in (a) fracture and (b) matrix at the end of the first year for the Mtest model.

Given the interest in the long–term thermal behavior, and the fact that there are no known large fractures, we only consider single-K models for further analysis.

The above discussion focuses on the temperature results for the vertical well layout. Another factor to be considered for the feasibility analysis is the reservoir impedance (RI), which is defined in this study as the pressure difference between the injection and production wells divided by the mass flow rate. Relative to initial hydrostatic reservoir pressure, the pressure increase at the injection well is about 11 ~ 14 MPa; The pressure drop at the production well is about 9 MPa, leading to a RI between 1.33 ~ 1.53 MPa s/kg (flow rate is ~ 15 kg/s).

3.3.2. Horizontal well layout

It is assumed the horizontal well is 500 m long at a depth of 2825 m in the base case scenario and fluid is injected over the length of 500 m. For a 10 cm radius well, the 15 kg/s flux comes out of an injection area of 314.2 ($2 \times \pi \times 0.1 \times 500$) m^2. In contrast, in the vertical well placement scenario, fluid is assumed to be injected over a 20 m perforated length within a 100 m thick reservoir, the 15 kg/s flux comes out of an injection area of 12.6 ($2 \times \pi \times 0.1 \times 20$) m^2. Because the injection area in the horizontal placement is 25 times more than it is in the vertical well placement, the local pressure increase due to fluid injection is much less. Similarly, the production area is much larger in the horizontal well placement. As a result, the reservoir volume that the fluid accesses is much larger than in the vertical well placement, as shown in Fig. 6. Because of the much greater access to rock volume, thermal breakthrough happens much later (i.e., around 40 years as shown in Fig. 7c homogeneous case, vs. 20 years for vertical wells shown in Fig. 2). Understandably, if the horizontal well is shorter, the breakthrough will happen earlier (e.g., a simulation shows the thermal breakthrough is at about 30 yr for a pair of 300 m long horizontal wells). At the end of 60 years of injection, the production temperature is still above 82 °C. Comparing to the vertical well placement, horizontal well placement clearly has two advantages: the thermal breakthrough is

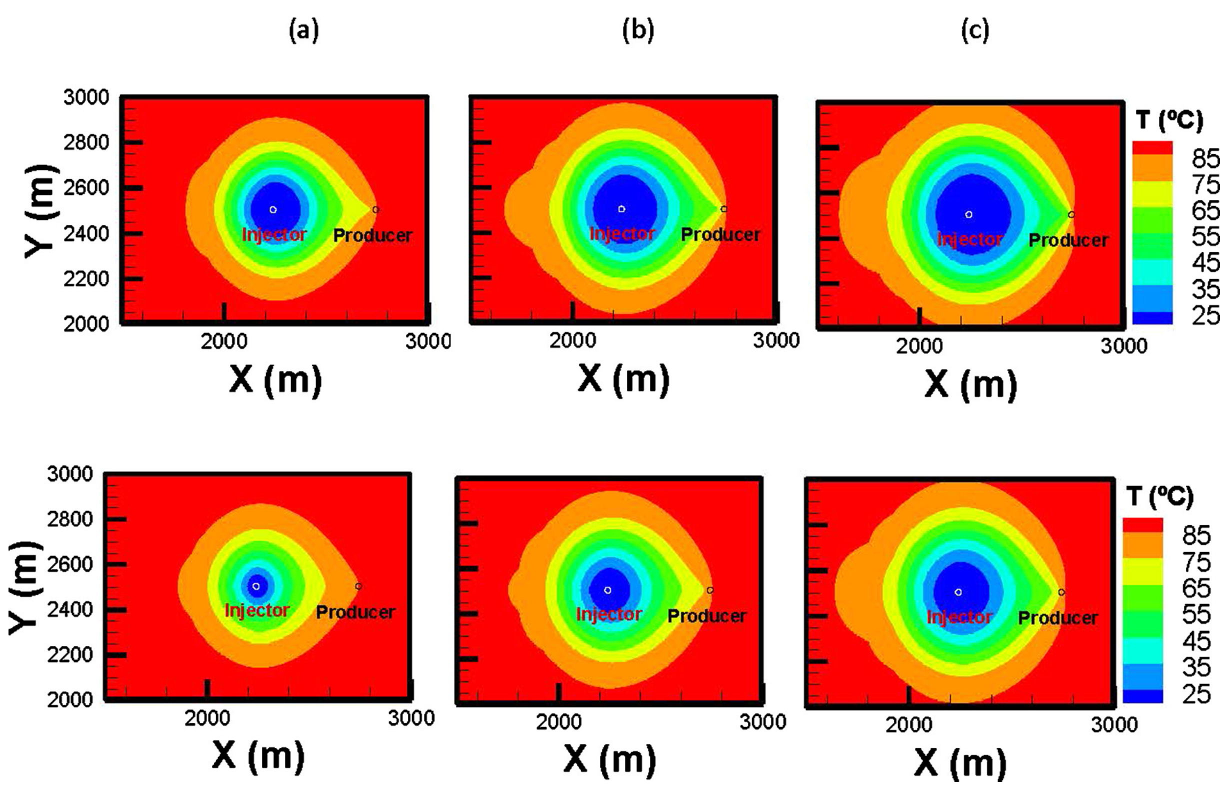

Fig. 5. Temperature distribution at the end of (a) 20 years; (b) 40 years; and (c) 60 years for the Mtest model. The upper panel shows temperature in fractures and lower panel shows temperature in matrix.

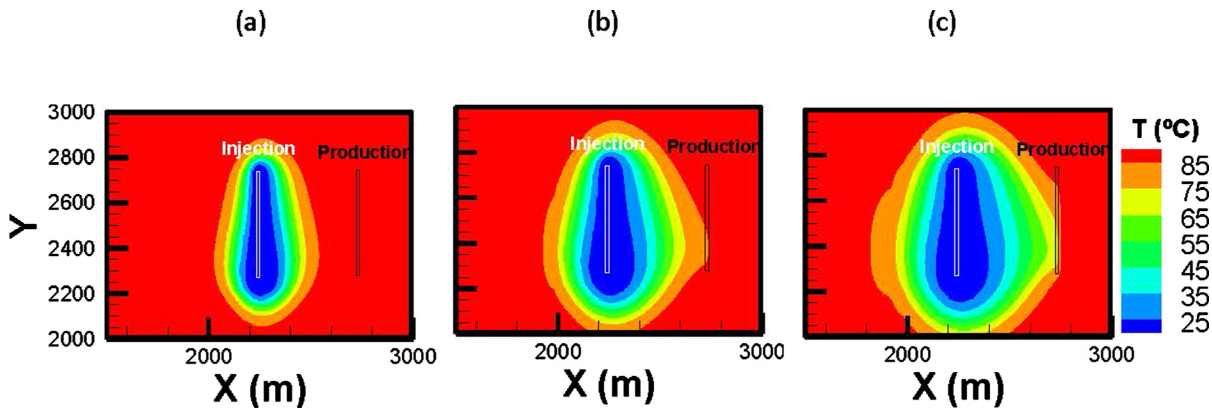

Fig. 6. Temperature distribution on an XY plane at an elevation where injection/production wells are perforated at (a) 20 years; (b) 40 years; and (c) 60 years.

later due to the much larger sweep area along the y direction; the pressure at the injection well bottom is much less, i.e., ~1 MPa vs. 14 MPa in the vertical well placement scenario, and the pressure drawdown needed at the production well is ~1 MPa vs. 9 MPa in the vertical well placement scenario. However, the drilling cost could be much higher for horizontal wells at such a depth. The economic implication of this work can be found in Garapati et al. (2019).

4. Impact of heterogeneity and uncertainty quantification (UQ)

Due to the lack of data and our incomplete knowledge, it is important to perform an uncertainty analysis to understand the potential range of model predictions, i.e., production temperature, and injection/production pressure difference. It is also important to understand which parameters contribute most to the prediction uncertainty so we can prioritize site characterization if a choice has to be made. Prediction uncertainty comes from two sources: model uncertainty and parameter uncertainty. We have already learnt from the previous section that the model predictions are not sensitive to the choice between a single-K model versus a dual-K model. In this section, we will explore how heterogeneity (which is unavoidable) as well as uncertain parameters may affect predictions.

4.1. Impact of heterogeneity

There is very little information on the heterogeneity of the formation. The way we tackle the lack of information is by starting with a couple of forward simulations with assumed parameters; then exploring the uncertainty in the predictions with assumed parameter uncertainty and identifying the most influential uncertainty parameter(s).

A heterogeneous permeability field is generated for the upper 2/3 of the formation using the GSLIB (Deutsch and Journel, 1992) implemented in iTOUGH2.

Because of the relatively large injection/production pressure difference encountered in the homogeneous model with the vertical well layout, we first examine how heterogeneity impacts reservoir pressure for the vertical well placement option. We start by performing a few forward simulations using different heterogeneous fields with vertical well placement, but even the smallest overpressure at the injection well can reach to almost ~30 MPa using these models, which is greater than hydrostatic pressure. In reality, such a high pressure could induce slip along pre-existing fracture critically oriented for shear reactivation or create hydraulic fractures, which makes vertical well pairs a non-option. For this reason, the rest of the investigation only focuses on horizontal well pair placement.

For horizontal well placement, the thermal breakthrough curve from a heterogeneous permeability field (shown in Fig. 7a) could also be very different from the homogeneous field (model discussed in section 3.3.2), as demonstrated in Fig. 7c. The reason is that heterogeneity could provide preferential flow paths, as shown in Fig. 7b, therefore, leading to earlier thermal breakthrough (i.e., ~ 10 year for this particular permeability field, as compared to 40 year for a homogeneous case). The example illustrates the importance of incorporating heterogeneity in the analysis.

4.2. Uncertainty quantification (UQ)

Since heterogeneity has such a substantial impact on model prediction, the discussion here will focus on the UQ analysis performed using a heterogeneous model. We performed two types of uncertainty analysis: 1. A First-Order-Second-Moment (FOSM) uncertainty propagation analysis to identify the most influential uncertain parameter on

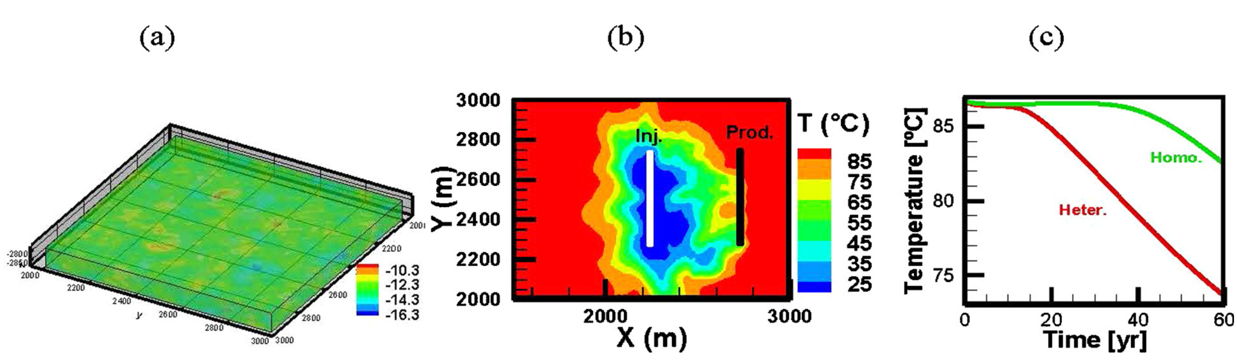

Fig. 7. (a) An example of permeability field (the center 1 km x 1 km) generated using the Sequential Gaussian Simulation (SGS) model with a correlation length of 100 m, the color scale indicates the logarithm of the permeability; (b) the temperature distribution at 60 years for the horizontal well layout from that permeability field; and (c) temperature BTC at the production well from this permeability field in red, as compared to the one from the previous homogeneous permeability field in green. (For interpretation of the references to colour in the Figure, the reader is referred to the web version of this article).

model predictions, the results of which can be used to help prioritize site characterization efforts; and 2. A formal Monte Carlo (MC) simulation that provides the potential uncertain range of the model predictions.

The uncertain parameters considered are: average permeability (formation upper 2/3), porosity, rock compressibility and seven parameters from GSLIB including correlation length (a range parameter indicating the distance within which a parameter is self-correlated), sill, rotation angles and anisotropy ratios, which characterize the heterogeneous permeability distribution. The simulations are performed using a fixed flow rate of 15 kg/s. The model predictions (outputs) are production temperature and injection/production pressure difference as an indication of RI for a fixed flow rate.

4.2.1. FOSM analysis

FOSM is the analysis of the mean and covariance of a random function (model output) based on its first order Taylor series expansion. It presumes that the mean and covariance are sufficient to characterize the distribution of the dependent variables. FOSM analysis relies on two assumptions: 1. Model outputs are normally distributed; and 2. perturbations about the mean can be approximated by linear functions. Because of the simplicity and low computational cost, FOSM can be used to provide preliminary uncertainty quantification and identify which parameters contribute more to the overall prediction uncertainty.

Table 3 shows the average contribution to model predictions from each uncertain parameter. This results clearly show that the correlation length contributes most (~ 43 %) to the uncertainty in both production temperature and pressure difference predictions. The other three parameters that stand out for uncertainty contributions are: permeability, porosity and sill (representing variance). This result further confirms that heterogeneous features have a large impact on production temperature and RI.

4.2.2. Monte Carlo simulations

The FOSM analysis provided the first order model prediction uncertainty based on certain assumptions and identified influential parameters. MC simulations do not rely on assumptions but are more computationally intensive. Here a MC simulation is performed considering all ten parameters listed in Table 3. Latin Hypercube sampling (LHS) (McKay et al., 1979; Zhang and Pinder, 2003) is used to ensure parameters are sampled within the parameter range and parameter distributions are reproduced (no parameter correlation is considered).

MC simulation results (Fig. 8) show that the average thermal breakthrough happens around 15 years for a heterogeneous field, although it could happen as early as 8 years, or as late as 30 plus years. The injection/production pressure difference is about 4 MPa on average, ranging from 2 ~ 8 MPa. Because very limited data exist on heterogeneity, or the parameters used to generate the heterogeneous field, the parameter sample range in the MC simulation is relatively large to be conservative. In addition, it is possible to have any parameter combination in generating the field due to lack of data suggesting otherwise. As a result, the prediction uncertainty is relatively large. Keep in mind only the solid line represents the average behavior from the MC simulation, the 95 and 5 percentile curves represent a very small percentage of simulations that are out of the range of the two curves, i.e., very small likelihood. The individual realizations are then entered into the economic model for the uncertainty in the economic prediction.

Table 3
Uncertainty parameters used in FOSM and their average contribution to model prediction uncertainty.

Parameter	Parameter range	Production temperature (%)	Injection/ production pressure difference (%)
Permeability	6.3e-15 ~ 1.e-13 m^2	12.40	25.87
Porosity	0.001 ~ 0.1	11.48	9.79
Compressibility	1.e-10 ~ 1.e-9	3.03	2.45
Correlation length	20 ~ 200 m	43.14	42.95
Rotation angle 1	0 ~ 90°	1.41	2.83
Rotation angle 2	0 ~ 90°	6.91	2.12
Rotation angle 3	0 ~ 90°	2.10	2.52
Anisotropy 1	1.0 ~ 10.0	0.93	0.6
Anisotropy 2	1.0 ~ 10.0	0.51	0.87
Sill	0.1 ~ 2.0	19.94	10.01

Since four influential parameters are identified by FOSM analysis (Table 3), further characterization to obtain information on these four parameters (i.e., reduce the uncertainty range of these four parameters) will help reduce this uncertainty in the prediction.

4.2.3. Uncertainty due to initial reservoir temperature or injected temperature

All previous simulations were performed using a geothermal gradient of 26 °C/km (Base case). To understand how initial reservoir temperature may affect production temperature decline, two additional scenarios using a higher geothermal gradient (HighG) of 30 °C/km, and a lower geothermal gradient (LowG) of 22 °C/km were simulated. As shown in Fig. 9, the thermal breakthrough curves are more or less shifted up and down, in parallel, for the three cases, although the final temperature drop (at 60 years) is a little more in the HighG case and a little less in the LowG case. These results demonstrate that once the initial reservoir temperature is obtained after wells are drilled in the field, if the actual reservoir temperature is not too far off from the scenarios considered in this study, the thermal predictions can be shifted accordingly.

Another factor that may impact the produced temperature is the initial injected temperature, which was assumed to be surface temperature 13.2 °C. Additional simulation is performed for an injected temperature of 45 °C, assuming the produced fluid is re-injected. The thermal breakthrough time is the same for the three scenarios investigated (horizontal well 500 m long, 300 m long, and vertical well setup). The difference is that the produced water temperature at the end of 60 years is slightly higher when 45 °C water is injected (e.g., 2 °C higher for the vertical well setup and less for the horizontal well setup). If the injected temperature is between 13.2 °C and 45 °C, the produced water temperature at a certain time can be interpolated from the two results.

5. Conclusions

In this study, we investigated the subsurface aspects of a potential Geothermal District Heating and Cooling system for West Virginia University Morgantown campus. Reservoir models were constructed to address the following questions:

- What is an appropriate model to use (single K vs. dual K) for thermal prediction at the production well? How does the model choice affect model prediction?
- We have constructed three models based on very limited field information, including one single-K model and two dual-K models (one based on fracture data received; another one represents a case with only a portion of large fractures conducting flow). Among the models investigated, single-K and the two dual-K models do not show much difference in thermal predictions. The thermal behavior at the production well is not sensitive to the model choices for this particular case because the relatively large distance between the injection/production wells (in all potential scenarios) leads to a long fluid residence time, therefore, the heat exchange between fracture and matrix is dominated by the matrix volume rather than heat exchange area between fracture and matrix. The model choice

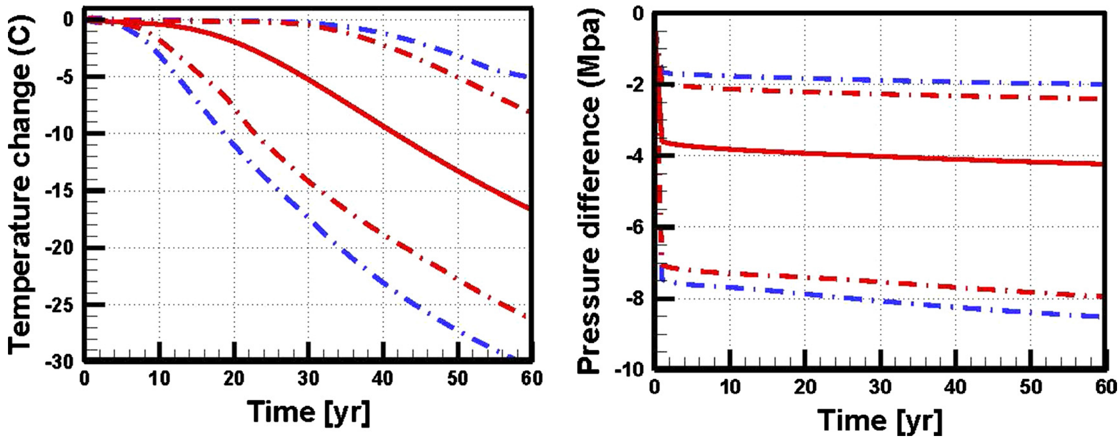

Fig. 8. Statistical estimate of (a) production temperature change and (b) production/injection pressure difference from the MC simulations. Red solid line indicates the mean prediction, red dashed lines indicate 95 and 5 percentiles and dashed blues lines are upper/lower bounds. (For interpretation of the references to colour in the Figure, the reader is referred to the web version of this article).

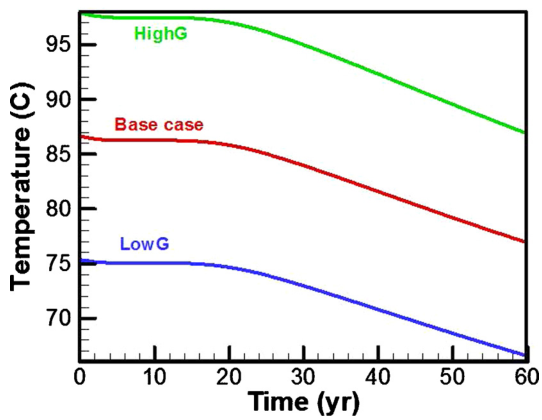

Fig. 9. Thermal breakthrough curves for a heterogeneous model with two horizontal well layout, using a high geothermal gradient 30 °C/km (HighG), base case geothermal gradient 26 °C/km, and a low geothermal gradient 22 °C/km (LowG).

between a single-K vs. a dual-K does not have much impact on the thermal prediction at the production well.

- What well placement choice should be considered?
- Two main well placement scenarios have been explored: a pair of horizontal wells vs. a pair of vertical wells. When the vertical well placement is used, the overpressure at the injection well with a heterogeneous field is too high (i.e., higher than fracturing pressure). As a result, the horizontal well option is considered for the rest of the study.
- What is the impact of heterogeneity? What is the uncertainty in the model predictions?
- Heterogeneity has a large impact model results, for both pressures and temperatures. The potential fast-flow paths could cause early thermal breakthrough. As a result horizontal well placement is a more robust design. The four most influential uncertain parameters are identified in the FOSM uncertainty analysis. Based on the Monte Carlo simulations, for the horizontal well placement option, the average thermal breakthrough could happen around 15 years, with a total temperature drop about 16 °C at the end of 60 years. The average pressure difference between the injection/production well pair is about 4 MPa.
- It is possible that the initial reservoir temperature is different than what is used in this study. Model results indicate if that is the case, the predicted thermal breakthrough curves can be shifted based on the difference between the actual and assumed initial temperature.

The model results can be further used as the inputs to the economic analysis.

Disclaimer

The information, data, or work presented herein was funded in part by an agency of the United States Government. Neither the United States Government nor any agency thereof, nor any of their employees, makes any warranty, express or implied, or assumes any legal liability or responsibility for the accuracy, completeness, or usefulness of any information, apparatus, product, or process disclosed, or represents that its use would not infringe privately owned rights. Reference herein to any specific commercial product, process, or service by trade name, trademark, manufacturer, or otherwise does not necessarily constitute or imply its endorsement, recommendation, or favoring by the United States Government or any agency thereof. The views and opinions of authors expressed herein do not necessarily state or reflect those of the United States Government or any agency thereof.

CRediT authorship contribution statement

Yingqi Zhang: Project administration, Funding acquisition, Investigation, Writing - original draft. **Nagasree Garapati:** Project administration, Funding acquisition, Investigation, Writing - review & editing. **Christine Doughty:** Investigation, Writing - review & editing. **Pierre Jeanne:** Investigation, Writing - review & editing.

Declaration of Competing Interest

The authors declare that they have no known competing financial interests or personal relationships that could have appeared to influence the work reported in this paper.

Acknowledgment

This manuscript is based upon work supported by the U.S. Department of Energy's Office of Energy Efficiency and Renewable Energy (EERE) under the Geothermal Technologies Office, under Award Number DE-EE0008105 to West Virginia University, and under Award Number DE-AC02-05CH11231 to the Lawrence Berkeley National Laboratory.

Appendix A. Supplementary data

Supplementary material related to this article can be found, in the online version, at doi:https://doi.org/10.1016/j.geothermics.2020.101848.

References

Aquaveo, 2013. LLC In Provo, Utah. GMS User Manual (v9.0) the Groundwater Modeling System.

Burns, E., Cladouhos, T.T., Williams, C.F., Bershaw, J., 2018. Controls on Deep Direct-Use Thermal Energy Storage (DDU-TES) in the Portland Basin 42 GRC Transactions, Oregon, USA.

Cornell University, 2017. Final Report: Low Temperature Geothermal Play Fairway Analysis for the Appalachian Basin. . https://gdr.openei.org/submissions/899.

Deutsch, C.V., Journel, A.G., 1992. GSLIB, Geostatistical Software Library and User's Guide. Oxford University Press, New York, New York.

Finsterle, S., 2004. Multiphase inverse modeling: review and iTOUGH2 applications. Vadose Zone J. 3.

Finsterle, S., Doughty, C., Kowalsky, M.B., Moridis, G.J., Pan, L., Xu, T., Zhang, Y., Pruess, K., 2008. Advanced vadose zone simulations using TOUGH. Vadose Zone J. 7, 601–609.

Garapati, N., Alonge, O.B., Hall, L., Irr, V.J., Zhang, Y., Smith, J.D., Jeanne, P., Doughty, C., 2019. Feasibility of development of geothermal deep direct-use district heating and cooling system at West Virginia university campus-Morgantown. In: WV. PROCEEDINGS, 44th Workshop on Geothermal Reservoir Engineering. Stanford University. Stanford, California.

Jóhannesson, T., 2015. Geothermal Experience in Iceland. Geothermal Direct Use Workshop Summary Report. . https://www.energy.gov/sites/prod/files/2015/09/f26/Geothermal%20Direct%20Use%20Workshop%20Summary%20Report%20-%20No%20List%20%2809-23-2015%29.pdf.

Major, M., Poulsen, S., Balling, N., 2018. A numerical investigation of combined heat storage and extraction in deep geothermal reservoirs. Geotherm. Energy 6 (1). https://doi.org/10.1186/s40517-018-0089-0.

McCleery, R.S., Moore, J.P., McDowell, R.R., Garapati, N., Carr, T.R., Anderson, B.J., 2018. Development of 3-D geological model of Tuscarora Sandstone for feasibility of deep direct-use geothermal at West Virginia university's main campus. GRC Transactions 42.

McDowell, R., 2018. Core Data Excel Sheet, Person Communication.

McKay, M.D., Conover, W.J., Beckman, R.J., 1979. A comparison of three methods for selecting values of input variables in the analysis of output from a computer code. Technometrics 21, 239–245.

Marcellus Shale Energy and Environment Laboratory (MSEEL). [dataset] DTS_Data.zip from Research – Well Datasets – Fiber Optics. 2018. http://mseel.org/Data/Wells_Datasets/MIP_3H/Fiber_Optics/DTS/DTS_Data.zip.

Patchen, D.G., et al., 2006. A Geologic Play Book for Trenton-black River Appalachian Basin Exploration, Final Report. NETL, DOE: West Virginia University Research Corp.

Pruess, K., Oldenburg, C., Moridis, G., 1999. *TOUGH2 user's guide, Version 2.0*, Report LBNL-43134. Lawrence Berkeley National Laboratory, Berkeley, CA.

Ryder, R.T., Crangle Jr., R.D., Trippi, M.H., Swezey, C.S., Lentz, E.E., Rowan, E.L., Hope, R.S., 2009. Geologic Cross Section D–D' Through the Appalachian Basin From the Findlay Arch, Sandusky County, Ohio, to the Valley and Ridge Province. U.S. Geological Survey Scientific Investigations Map 3067, Hardy County, West Virginia 2 sheets, 52-p. pamphlet.

Ryder, R., Zagorski, W., 2003. Nature, origin, and production characteristics of the Lower Silurian regional oil and gas accumulation, central Appalachian basin, United States. Bull. 87 (5), 847–872 2.

Smith, J.D., 2016. Analytical and Geostatistical Heat Flow Modeling for Geothermal Resource Reconnaissance Applied in the Appalachian Basin. Cornell University, pp. 254 MS Thesis.

Tester, J., 2015. Geothermal Deep Direct Use Technology. Geothermal Direct Use Workshop Summary Report.

Whealton, C.A., Stedinger, J.R., Horowotiz, F.G., 2015. Application of generalized least squares regression in bottom-hole temperature corrections. Final Report: Low Temperature Geothermal Play Fairway Analysis for the Appalachian Basin. pp. 130–144.

Zhang, Y., Pinder, G., 2003. Latin hypercube lattice sample selection strategy for correlated random hydraulic conductivity fields. Water Resour. Res. 39 (8), 1226. https://doi.org/10.1029/2002WR001822.

Zhang, Y., Pan, L., Pruess, K., Finsterle, S., 2011. A time-convolution approach for modeling heat exchange between a wellbore and surrounding formation. Geothermics 40 (4), 261–266. https://doi.org/10.1016/J.GEOTHERMICS.2011.08.003.

Zhou, Q., Oldenburg, C.M., Rutqvist, J., 2019. Revisiting the analytical solutions of heat transport in fractured reservoirs using a generalized multirate memory function. Water Resour. Res. 55, 1405–1428. https://doi.org/10.1029/2018WR024150.